Fourier Transform Infrared Spectroscopy of Electrogenerated Anions and Cations of Metal-Substituted Bacteriochlorophyll *a*

G. Hartwich,[†] C. Geskes,[‡] H. Scheer,[§] J. Heinze,[‡] and W. Mäntele*,[⊥]

Contribution from the Institut für Physikalische und Theoretische Chemie, Technische Universität München, 85748 Garching, Germany, Institut für Physikalische Chemie, Universität Freiburg, 79104 Freiburg, Germany, Botanisches Institut der Universität, 80638 München, Germany, and Institut für Biophysik and Strahlenbiologie, Universität Freiburg, 79104 Freiburg, Germany

Received December 28, 1994[⊗]

Abstract: The monoanions (the terms monoanions (anions) and monocations (cations) used in this paper refer to π-monoanion radical and π-monocation radical, respectively) and monocations of transmetalated bacteriochlorophyll *a* [M]-BChla (M = Mn, Zn, Cd, Co, Ni, Cu, Pd) and the corresponding 13^2-hydroxy derivatives [M]-OH-BChla were investigated by a combination of Fourier transform infrared (FTIR) spectroscopy and electrochemistry between 1800 and 1200 cm^{-1}. [M]-BChla undergoing only ring-centered redox processes (M = Zn, Cd, Ni, Cu, and Pd) exhibit FTIR difference spectra typical for the monoanions [M]-BChla$^{\bullet-}$ and for the monocations [M]-BChla$^{\bullet+}$. The exceptions are the Ni derivatives and the monocations of the Co derivatives. They are attributed to a deformation of the bacteriochlorin macrocycle from a planar toward a nonplanar conformer. [M]-BChla undergoing metal-centered redox processes (M = Mn, Co) resemble the FTIR difference spectra of the [M]-BChla undergoing ring-centered redox processes in the carbonyl frequency region and below 1400 cm^{-1}, where the main contributions arise from C−N and C−C modes. The skeletal modes between 1400 and 1600 cm^{-1} are strongly influenced by the metal-centered redox reactions. The 13^2-ester absorption and difference band is proposed as a marker band for distortions of the planar macrocycle toward a nonplanar conformer.

Introduction

In bacterial photosynthetic reaction centers (RC), an electron is transferred upon excitation with light from a special pair of bacteriochlorophyll molecules (BChl; for structure, see Figure 1) to a quinone electron acceptor, thus creating a charge-separated state which stores a substantial fraction (approximately 40%) of the incoming photon energy.[2] The high-resolution X-ray structures of protein crystals, available from RC of *Rhodopseudomonas viridis*[3] and *Rhodobacter sphaeroides*,[4] provide information on the spatial arrangement of the cofactors and the protein part and suggest distinct electron transfer pathways in the cofactor array as well as specific pigment−protein interactions. However, the structures derived from crystallography only represent a static picture of the relaxed RC in the crystal form and cannot account for all aspects of the dynamic process of electron transfer.

Electron transfer starts from the special pair (P) and leads to reduction of a bacteriopheophytin (BPheo) (H) molecule within approximately 3 ps. From there, the electron is transferred to a primary quinone electron acceptor (Q_A). An ongoing debate

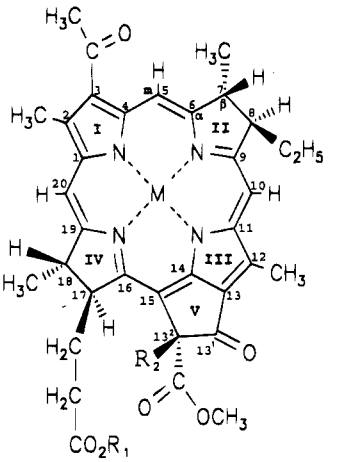

Figure 1. Structure of transmetalated bacteriochlorophyll *a* ([M]-BChla) and the respective 13^2-hydroxy derivatives ([M]-OH-BChla) (M = metal; R_1 = phytol $C_{20}H_{39}$; R_2 = H, OH).

is whether the monomeric BChl (B) located between the special pair and the BPheo is involved as a redox intermediate. In this case, a sequential electron transfer model (P → B → H → Q_A) applies, whereas a model involving direct electron transfer from P to H (P → H → Q_A) could only be explained by a superexchange mechanism.[5] At present, ultrafast time-resolved spectroscopic measurements from different groups have been reported as supportive for[6] or against[7] a sequential electron transfer involving the intermediate B. The search for an intermediate B^- in the picosecond domain, barely populated because of comparable rates for formation and decay,[8] is

* To whom correspondence should be addressed at the Institut für Physikalische und Theoretische Chemie, Universität Erlangen, Egerlandstrasse 3, 91058 Erlangen, Germany.
[†] Technische Universität München.
[‡] Institut für Physikalische Chemie, Universität Freiburg.
[§] Botanisches Institut der Universität.
[⊥] Institut für Biophysik und Strahlenbiologie, Universität Freiburg.
[⊗] Abstract published in *Advance ACS Abstracts,* July 1, 1995.

(1) The terms monoanions (anions) and monocations (cations) used in this paper refer to p-monoanion radical and p-monocation radical, respectively.

(2) Parson, W. W. *Annu. Rev. Biophys. Bioeng.* **1982**, *11*, 57.
(3) (a) Michel, H.; Epp, O.; Deisenhofer, J. *EMBO J.* **1986** *5*, 2445. (b) Deisenhofer, J.; Epp, O.; Miki, K.; Huber, R.; Michel, H. *J. Mol. Biol.* **1984**, *180*, 385.
(4) (a) Allen, J. P.; Feher, G.; Yeates, T. O.; Rees, D. C.; Deisenhofer, J.; Michel, H.; Huber, R. *Proc. Natl. Acad. Sci. U.S.A.* **1986**, *83*, 8589. (b) Chang, C. H.; Tiede, D.; Tang, J.; Smith, U.; Norris, J.; Schiffer, M. *FEBS Lett.* **1986**, *205*, 82. (c) Chang, C. H.; El-Kabbani, O.; Tiede, D.; Norris, J.; Schiffer, M. *Biochemistry* **1991**, *30*, 5352.
(5) (a) Marcus, R. A. *Chem. Phys. Lett.* **1987**, *133*, 471. (b) Michel-Beyerle, M. E.; Bixon, M.; Jortner, J. *Chem. Phys. Lett.* **1988**, *151*, 188. (c) Michel-Beyerle, M. E.; Plato, M.; Deisenhofer, J.; Michel, H.; Bixon, M.; Jortner, J. *Biochim. Biophys. Acta* **1988**, *932*, 52 and references therein.
(6) (a) Holzapfel, W.; Finkele, U.; Kaiser, W.; Oesterhelt, D.; Scheer, H.; Stilz, H.; Zinth, W. *Proc. Natl. Acad. Sci. U.S.A.* **1990**, *87*, 5168. (b) Dressler, K.; Umlauf, E.; Schmidt, S.; Hamm, P.; Zinth, W.; Buchanan, S.; Michel, H. *Chem. Phys. Lett.* **1991**, *183*, 270.

0002-7863/95/1517-7784$09.00/0 © 1995 American Chemical Society

severely hampered by the considerable overlap of the electronic levels of P, P*, P^+, B, B^-, H, and H^- in the UV/vis/near-IR spectral region.

An approach to facilitate the separation of electronic transitions which are specific for B^- was the extraction of the monomeric BChl from the RC and its substitution by chemically modified analogs.[9] In RC with [3-vinyl]-13^2-hydroxy-BChla the absorption bands of B are shifted compared to the native BChla transitions. Ultrafast time-resolved measurements of this RC have shown a decrease of the primary electron transfer rate by a factor of 10, thus indicating the participation of the substituted monomeric BChla in electron transfer.[10]

Another possibility to modify the spectral and electron transfer properties of BChl is the replacement of the central magnesium by other metals.[11] This transmetalation is supposed to alter the redox properties and thus the driving force for the primary electron transfer steps. In addition, spectral modifications are expected, in particular in the 500−600 nm region. In another paper, we have described the redox potentials and electronic absorption spectra of the neutral, anion, and cation forms for several transmetalated BChla ([M]-BChla) species.[12]

Since it is expected that the replacement of Mg by other central metals not only changes the electronic levels and the redox properties but can also affect the entire conformation of the macrocycle, a detailed structural analysis of these pigments is necessary. Vibrational infrared (IR) spectroscopy can be used to assess the planarity and deformation of the macrocycle and the conformation of the pigment side groups. In previous investigations combining electrochemistry and IR spectroscopy,[13] the effect of anion or cation formation on the vibrational spectrum was analyzed for isolated native pigments such as BChla and Chla in organic solvents and compared to the properties of the pigments *in situ*. Since ultrafast time-resolved measurements on photosynthetic RC have recently been extended to the picosecond time domain in the IR,[14] an analysis of the vibrational modes of the anion and cation radical forms of transmetalated pigments can also provide a basis for the assignment of vibrational bands of B^- in the RC.

We present here the vibrational analysis of monoanion and monocation formation of several metal-substituted bacteriochlorophyll *a* [M]-BChla (M = Mn, Zn, Cd, Co, Ni, Cu, Pd) and their respective 13^2-hydroxy derivatives [M]-OH-BChla.

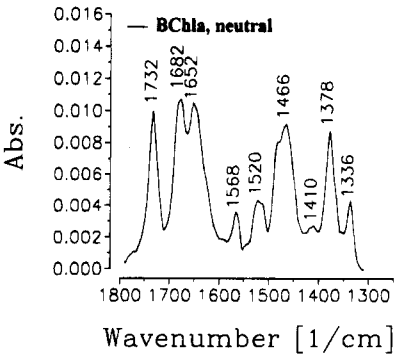

Figure 2. FTIR absorption spectrum of bacteriochlorophyll *a* (BChla) in THF ($c = 6 \times 10^{-3}$ M). Conditions: $T = 5$ °C; 64 interferograms added; resolution 4 cm^{-1}.

Materials and Methods

Pigments were prepared as described by Hartwich et al.[11]

The solvent tetrahydrofuran (THF) (Fluka, HPLC grade) was purified by distillation with Na/K alloy under nitrogen for 2 h. Tetrabutylammonium hexafluorophosphate ($TBAPF_6$) was used as the electrolyte (0.3 M). It was purified according to a procedure described elsewhere.[15]

All measurements were carried out in a specially designed IOTTLE cell (infrared and optical transparent thin layer electrochemical cell) described elsewhere.[16] The cell was used at a path length of 55 μm and allowed measurements in the UV/vis/IR spectral range (190−10000 nm). It is equipped with a three-electrode configuration for constant potential electrolysis (CPE). The working electrode was a 6 μm gold minigrid (Buckbee-Mears Co., St. Paul, MN) sputtered with Pt. A Pt sheet was used as the counter electrode, and a Ag wire served as the reference electrode. Potentials were calibrated against cobaltocene (−0.96 V vs Ag/AgCl). All potentials are quoted vs Ag/AgCl.

IR spectra were recorded on a Bruker IFS 25 FTIR spectrometer equipped with a MCT detector for high sensitivity. The optical setup was modified to provide a second measuring beam for vis/near-IR spectra in the range between 400 and 1100 nm for the control of the redox state. CPE as well as the vis/near-IR and IR spectra was controlled from software ("MSPEK") developed by S. Grzybek in our laboratory.

Redox-induced difference spectra were obtained by first equilibrating the sample at the initial potential for several minutes and then recording the vis/near-IR and IR single beam spectra. Then the potential was stepped 200 mV beyond the redox potential of the monocation or monoanion of the sample. After the decay of the current to zero, the vis/near-IR and IR spectra of the final state were recorded. The solvent and electrolyte bands were subtracted from the absorption spectra by use of a blank spectrum obtained with the same cell.

All spectra were recorded at 5 °C.

Results

The FTIR absorption spectrum of neutral BChla is shown in Figure 2. In general, the IR spectrum of BChla between 1800 and 1200 cm^{-1} was divided into three frequency regions. In the region between 1600 and 1750 cm^{-1}, the carbonyl group frequencies of BChla contribute. The absorption band at 1732 cm^{-1} is assigned to the 13^2- and 17^2-ester groups, which are degenerate in native BChla. The band at 1682 cm^{-1} is due to the 13^1-keto group of the isocyclic ring V of BChla, and the band at 1652 cm^{-1} to the 3-acetyl group. All reported positions are characteristic for noninteracting groups as is expected for the non-hydrogen-bonding solvent THF used in our experiments.[17] In the frequency region between 1400 and 1600 cm^{-1}, the C=C, C=N, and C−C modes of the macrocycle appear.

(7) (a) Hamm, P.; Gray, K. A.; Oesterhelt, D.; Feick, R.; Scheer, H.; Zinth, W. *Biochim. Biophys. Acta* **1993**, *1142*, 99. (b) Martin, J. L.; Breton, J.; Hoff, A. J.; Antonetti, A. *Proc. Natl. Acad. Sci. U.S.A.* **1986**, *83*, 957. (c) Wasielewski, M. R.; Tiede, D. M. *FEBS Lett.* **1986**, *204*, 368. (d) Kirmaier, C.; Holten, D. *Proc. Natl. Acad. Sci. U.S.A.* **1990**, *87*, 3552.

(8) Arlt, T.; Schmidt, S.; Kaiser, W.; Lauterwesser, C.; Meyer, M.; Scheer, H.; Zinth, W. *Proc. Natl. Acad Sci. U.S.A.* **1993**, *90*, 11757.

(9) (a) Struck, A.; Scheer, H. *FEBS Lett.* **1990**, *261*, 385. (b) Struck, A.; Cmiel, E.; Katheder, I.; Scheer, H. *FEBS Lett.* **1990**, *268*, 180. (c) Scheer, H.; Struck, A. In *The Photosynthetic Reaction Center*; Deisenhofer, J., Norris, J. R., Eds.; Academic Press: San Diego, 1993; Vol. 1, p 157.

(10) Finkele, U.; Lauterwasser, C.; Struck, A.; Scheer, H.; Zinth, W. *Proc. Natl. Acad. Sci. U.S.A.* **1992**, *89*, 9514.

(11) Hartwich, G.; Cmiel, E.; Katheder, I.; Schäfer, W.; Scherz, A.; Scheer, H. *J. Am. Chem. Soc.*, in press.

(12) Geskes, C.; Hartwich, H.; Scheer, H.; Mäntele, W.; Heinze, J. *Inorg. Chem.*, submitted for publication.

(13) (a) Mäntele, W.; Leonhard, M.; Bauscher, M.; Nabedryk, E.; Breton, J.; Moss, D. A. In *Reaction Centers of Photosynthetic Bacteria*; Michel-Beyerle, M.-E., Ed.; Springer: Berlin, 1990; p 31. (b) Nabedryk, E.; Leonhard, M.; Mäntele, W.; Breton, J. *Biochemistry* **1990**, *23*, 3242. (c) Mäntele, W.; Wollenweber, A.; Rashwan, F.; Heinze, J.; Nabedryk, E.; Berger, G.; Breton, J. *Photochem. Photobiol.* **1988**, *47*, 451. (d) Mäntele, W.; Wollenweber, A.; Nabedryk, E.; Breton, J. *Proc. Natl. Acad. Sci. U.S.A.* **1988**, *85*, 8468. (e) Mäntele, W.; Leonhard, M.; Bauscher, M.; Nabedryk, E.; Berger, B.; Breton, J. In *Molecular Biology of Membrane-Bound Complexes in Phototrophic Bacteria*; Drews, G., Ed.; Plenum Press, New York: 1990; p 313.

(14) (a) Maiti, S.; Cowen, B.; Diller, R.; Iannone, M.; Moser, C.; Dutton, P. L.; Hochstrasser, R. *Proc. Natl. Acad. Sci. U.S.A.* **1993**, *90*, 5247. (b) Walker, G. C.; Maiti, S.; Cowen, B. R.; Moser, C. C.; Dutton, P. L.; Hochstrasser, R. M. *J. Phys. Chem.* **1994**, *98*, 5778. (c) Hamm, P.; Zurek, M.; Mäntele, W.; Mayer, M.; Scheer, H.; Zinth, W. *Proc. Natl. Acad. Sci. U.S.A.* **1995**, *92*, 1826.

(15) Süttinger, R. Ph.D. Thesis, Universität Freiburg, Germany, 1980.

(16) Bauscher, M.; Nabedryk, E.; Bagley, K.; Breton, J.; Mäntele, W. *FEBS Lett.* **1990**, *261*, 191.

They are coupled and thus are difficult to assign. These modes are strongly influenced by substitution of the central metal, as shown by resonance Raman (RR) examinations of various porphyrin systems[18] and metal-substituted chlorophyll *a* ([M]-Chla).[19] At frequencies below 1400 cm^{-1}, contributions arise mainly from the C−H bending modes and the C−N vibrations.

In the FTIR difference spectra of electrogenerated monoanions and monocations of BChla and the transmetalated derivatives, negative bands arise from the disappearance of modes of the neutral molecule, whereas positive bands are due to formation of the anion or cation species, respectively. We will characterize negative bands in the FTIR difference spectra with (−) and positive bands with (+). For a better representation, we have recorded the difference spectra twice, first after complete monoanion or monocation formation and then after the reoxidation or rereduction to the neutral species, respectively. We also report the corresponding vis/near-IR absorption spectra. The multiple (>10) isosbestic points, seen in the FTIR difference spectra, indicate that only two species (neutral and radical ion) are present, and byproducts or reaction products from the radicals can be neglected.

Since the macrocycle vibrations are very complicated to assign, we only confer to band assignments which are unequivocal under the experimental conditions.

Neutral-minus-Anion FTIR Difference Spectra. Parts a and b of Figure 3 show the representative FTIR absorption spectra of the neutral and monoanion species as well as the FTIR neutral-minus-anion difference spectrum after electrolysis and the anion-minus-neutral difference spectrum after reoxidation of [Cu]-BChla. Table 1 lists the main FTIR difference bands of the examined derivatives.

The monoanion formation of [Cu]-BChla is accompanied by drastic changes in the region from 1600 to about 1750 cm^{-1}. In the absorption spectrum, the ester bands are shifted from 1734 cm^{-1} (neutral species) to 1730 cm^{-1} (anion). This results in a difference band at 1738(−)/1724(+) cm^{-1}. The 13^1-keto absorption band at 1690 cm^{-1} vanishes, as does the 3-acetyl band (1654 cm^{-1}). A new strong double band appears in the anion at 1646 and 1624 cm^{-1}. In the difference spectrum, the corresponding band (1690 cm^{-1}) and positive difference bands (1646 and 1624 cm^{-1}) are observed. Most prominent in the 1600−1400 cm^{-1} frequency region is the disappearance of absorption bands at 1554 and 1538 cm^{-1}. The difference spectrum shows the expected two negative bands at 1554 and 1540 cm^{-1}, and in addition positive difference bands at 1488 and 1452 cm^{-1}. Below 1400 cm^{-1}, the absorption spectrum of the neutral species shows three bands at 1380, 1364, and 1330 cm^{-1}. These bands are enhanced and partially shifted in the anion absorption spectrum. In the difference spectrum, three positive bands at 1382, 1362, and 1328 cm^{-1} are observed.

The obtained neutral-minus-anion difference spectra of all examined derivatives are similar to the one of [Cu]-BChla shown in Figure 2b. A downshift for all carbonyl frequencies is observed. In general, the ester band is shifted toward higher frequencies by 6−16 cm^{-1} for the [M]-OH-BChla compared to the unsubstituted derivatives, whereas the 13^1-keto band is only slightly shifted toward higher frequencies in the [M]-OH-BChla.

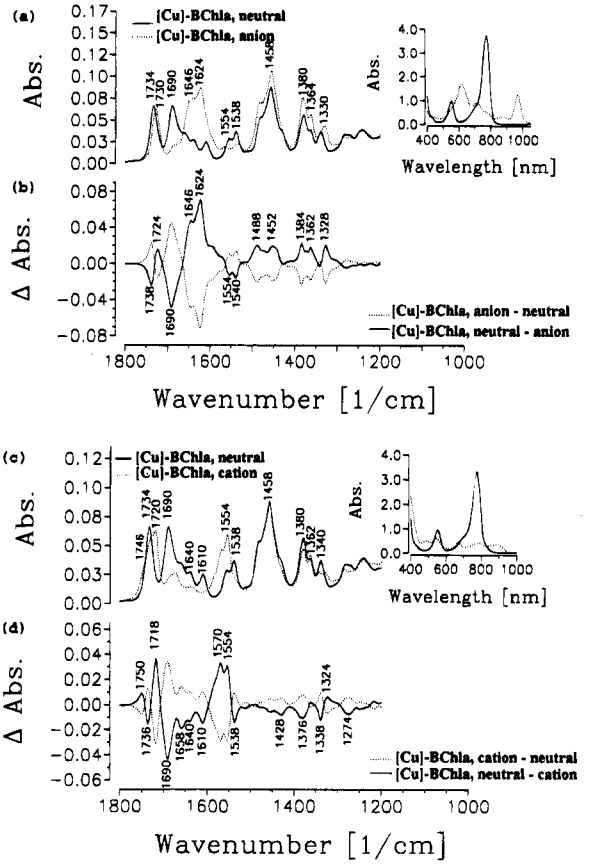

Figure 3. (a) FTIR absorption spectra of the neutral [Cu]-BChla (c = 5 × 10^{-3} M) and the fully evolved anion species after electrolysis at −1.4 V vs Ag/AgCl. (b) FTIR difference spectra ([Cu]-BChla minus [Cu]-BChla anion) for the anion formation after electrolysis and after increasing the voltage to −0.3 V vs Ag/AgCl. Inset: corresponding vis/near-IR absorption spectra of the neutral species (solid line) and the anion (dashed line) of [Cu]-BChla. (c) FTIR absorption spectra of [Cu]-BChla and the fully evolved cation after electrolysis at 0.65 V vs Ag/AgCl. (d) FTIR difference spectra ([Cu]-BChla minus [Cu]-BChla cation) after electrolysis at 0.65 V vs Ag/AgCl and after decreasing the voltage to −0.3 V vs Ag/AgCl. Inset: corresponding vis/near-IR absorption spectra of the neutral species (solid line) and the cation (dashed line) of [Cu]-BChla. Conditions for (a)−(d): T = 5 °C; 64 interferograms added; resolution 4 cm^{-1}.

Major deviations from the described typical difference spectrum of [Cu]-BChla were observed for the Ni derivatives. The absorption spectrum of [Ni]-OH-BChla shows a split 13^2-ester band at 1732 and 1746 cm^{-1} (Figure 4, inset 2). Figure 4a shows the neutral-minus-anion difference spectrum of [Ni]-OH-BChla. The ester difference band (1754(−)/1736(+)) is upshifted by 8−10 cm^{-1} relative to the other bands in [M]-OH-BChla.[20] A clearly separated difference band at 1696(−)/1666(+) cm^{-1} for the [Ni]-OH-BChla appears (1696(−)/1670(+) cm^{-1} for [Ni]-BChla). In the case of [Ni]-BChla, a broadened ester band appears in the absorption spectrum that is composed of two superimposed bands. A shoulder at 1748 cm^{-} in the difference spectrum appears at higher frequencies than the main difference band at 1738 cm^{-1}.

As reported,[12] the Co derivatives are reduced at the central metal instead of being reduced at the ring. In the carbonyl frequency region (Figure 5a), separated difference bands at 1686(−)/1664(+) cm^{-1} for [Co]-BChla and 1694(−)/1672(+) cm^{-1} for [Co]-OH-BChla are observed. The other difference

(17) Ballschmiter, K.; Katz, J. J. J. *Am. Chem. Soc.* **1969**, *91*, 2661.
(18) (a) Kitagawa, T.; Ogoshi, H.; Watanabe, E.; Yoshida, Z.-I. *J. Phys. Chem.* **1975**, *79*, 2629. (b) Spauling, L. D.; Chang, C. C.; Yu, N.-T.; Felton, R. H. *J. Am. Chem. Soc.* **1975**, *97*, 2517. (c) Ogoshi, H.; Watanabe, E.; Yoshida, Z.; Kincaid, J.; Nakamoto, K. *Inorg. Chem.* **1975**, *14*, 1344. (d) Spiro, T. G.; Stong, J. D.; Stein, P. *J. Am. Chem. Soc.* **1979**, *101*, 2648. (e) Kincaid, J. R.; Urban, M. W.; Watanabe, T.; Nakamoto, K. *J. Phys. Chem.* **1983**, *87*, 3096.
(19) (a) Fujiwara, M.; Tasumi, M. *J. Phys. Chem.* **1986**, *90*, 250. (b) Fujiwara, M.; Tasumi, M. *J. Phys. Chem.* **1986**, *90*, 5646.

(20) The identical upshift is also seen for [Cu]-OH-BChla. As mentioned in the preceding paper in this issue, we speculated that this is due to a deformation of the macrocycle, as described later in this paper for the Ni derivatives.

Table 1. Frequencies of the FTIR Neutral-minus-Anion Difference Spectra of [M]-BChla and [M]-OH-BChla[a]

compound	13^2-ester	13^1-keto	carbonyl frequencies			skeletal modes			C−H and C−N modes		
BChla[b]	1740(−)/1724(+)	1683(−)	1643(+)	1620(+)	1592(+)	1568(−)	1478(+)	1438(+)	1378(+)	1340(−)	1327(+)
[Mn]-OH-BChla	1742(−)/1720(+)	1680(−)		1634(+)	1608(+)	1514(−)	1464(+)	1420(+)	1370(+)	1346(+)	1322(+)
[Mn]-BChla	1742(−)/1716(+)	1680(−)		*d*	*d*	1512(−)	1478(+)	1420(+)	1376(+)	1344(+)	1324(+)
[Zn]-OH-BChla	1744(−)/1726(+)	1690(−)		1640(+)	1606(+)	1522(−)	1474(+)	1432(+)	1382(+)	1352(+)	1326(+)
[Zn]-BChla	1736(−)/1720(+)	1686(−)		1624(+)	1608(+)	1520(−)	1474(+)	1438(+)	1380(+)	1350(+)	1324(+)
[Cd]-OH-BChla	1744(−)/1724(+)	1688(−)		1636(+)	1606(+)	1528(−)	1462(−)	1430(+)	1372(+)	1348(+)	1324(+)
[Cd]-BChla	1736(−)/1722(+)	1682(−)		1622(+)	1612(+)	1524(−)	1460(−)	1428(+)	1374(+)	1348(+)	1324(+)
[Ni]-OH-BChla	1754(−)/1736(+)	1696(−)	1666(+)	1640(+)	1626(+)	1548(−)	1480(+)	1430(+)	1380(+)	1358(+)	1326(+)
[Ni]-BChla	1748(−),1738(−)/1718(+)[c]	1696(−)	1670(+)	*d*	1626(+)	1542(−)	1482(+)	1428(+)	1386(+)	1360(+)	1332(+)
[Co]-OH-BChla	1746(−)/1720(+)	1694(−)	1672(+)	1628(+)	1586(+)	1540(−)	1506(+)	1466(+)	1388(+)	1360(+)	1328(+)
[Co]-BChla	1738(−)/1724(+)	1686(−)	1664(+)	1632(+)	1586(+)	1544(−)	1504(+)	1468(+)	1388(+)	1362(+)	1322(+)
[Cu]-OH-BChla	1754(−)/1734(+)	1692(−)		1644(+)	1622(+)	1554(−)	1484(+)	1444(+)	1384(+)	1362(+)	1328(+)
[Cu]-BChla	1738(−)/1724(+)	1690(−)		1646(+)	1624(+)	1554(−)	1488(+)	1452(+)	1384(+)	1362(+)	1328(+)
[Pd]-OH-BChla	1746(−)/1726(+)	1698(−)		1648(+)	1618(+)	1562(−)	1482(+)	1454(+)	1386(+)	1368(+)	1332(+)
[Pd]-BChla	1746(−)/1728(+)	1698(−)		1648(+)	1618(+)	1562(−)	1484(+)	1452(+)	1386(+)	1370(+)	1332(+)

[a] All band positions are in inverse centimeters. [b] Data taken from ref 13c. [c] Superposition of two difference bands. [d] Only weak difference band observed.

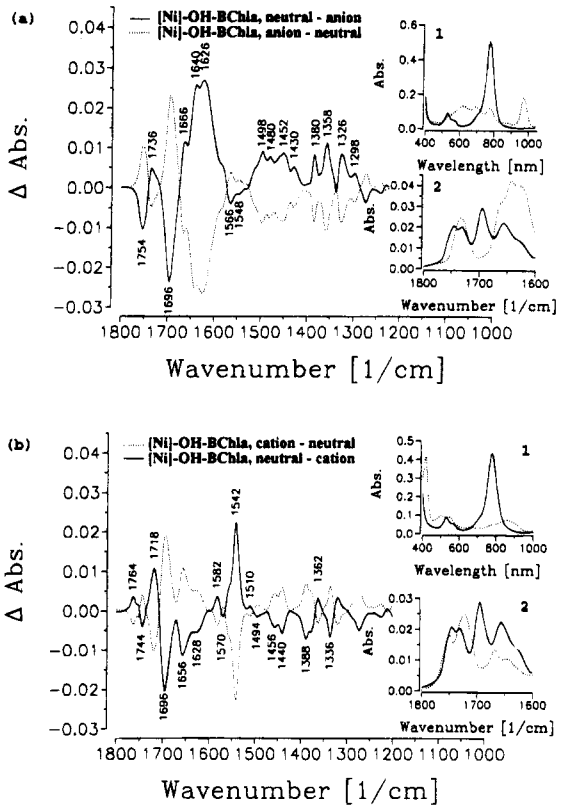

Figure 4. (a) FTIR difference spectra ([Ni]-OH-BChla minus [Ni]-OH-BChla anion) ($c = 10^{-3}$ M) after electrolysis at −1.2 V vs Ag/AgCl and after increasing the voltage to −0.3 V vs Ag/AgCl. Inset 1: Corresponding vis/near-IR absorption spectra for the neutral species (solid line) and the anion (dashed line). Inset 2: Corresponding FTIR absorption spectra for the neutral species (solid line) and the anion (dashed line) in the range between 1600 and 1800 cm^{-1}. (b) FTIR difference spectra ([Ni]-OH-BChla minus [Ni]-OH-BChla cation) after electrolysis (solid line) at 0.55 V vs Ag/AgCl and after decreasing the voltage to −0.3 V vs Ag/AgCl (dashed line). Inset 1: Corresponding vis/near-IR absorption spectra for the neutral species (solid line) and the cation (dashed line). Inset 2: Corresponding FTIR absorption spectra for the neutral species (solid line) and the cation (dashed line) in the range between 1600 and 1800 cm^{-1}. Conditions for (a) and (b): $T = 5$ °C; 64 interferograms added; resolution 4 cm^{-1}.

bands in the carbonyl region and the difference bands below 1400 cm^{-1} follow the described band pattern of anion formation. The skeletal modes are considerably different from those of the other derivatives. For [Co]-OH-BChla, two negative bands at 1566 and 1544 cm^{-1} and two strong positive difference bands at 1504 and 1468 cm^{-1} appear.

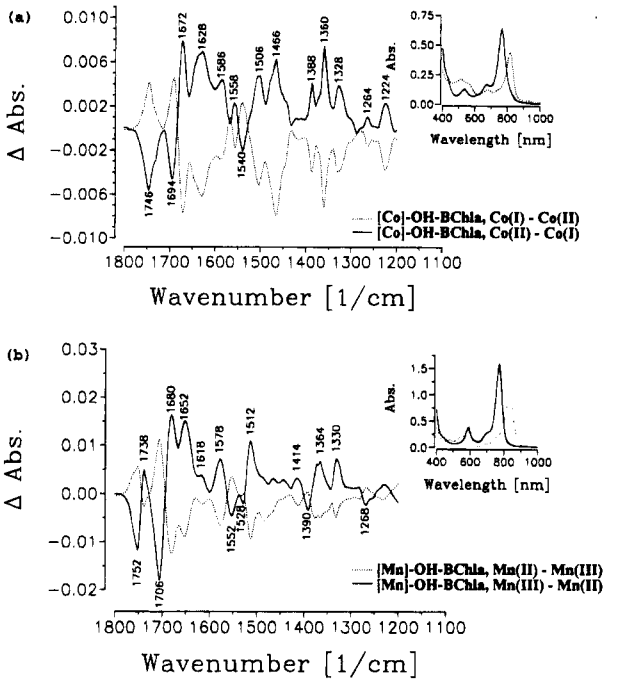

Figure 5. (a) FTIR difference spectra ([Co(II)]-OH-BChla minus [Co(I)]-OH-BChla anion) ($c = 1.5 \times 10^{-3}$ M) after electrolysis at −1.4 V vs Ag/AgCl and after increasing the voltage to −0.3 V vs Ag/AgCl. Inset: Corresponding vis/near-IR absorption spectra for the neutral species (solid line) and the anion (dashed line). (b) FTIR difference spectra ([Mn]-OH-BChla minus [Mn]-OH-BChla cation) ($c = 3 \times 10^{-3}$ M) after electrolysis (solid line) at 0.3 V vs Ag/AgCl and after decreasing the voltage to −0.5 V vs Ag/AgCl (dashed line). Inset: Corresponding vis/near-IR absorption spectra for the neutral species (solid line) and the anion (dashed line). Conditions for (a) and (b): $T = 5$ °C; 64 interferograms added; resolution 4 cm^{-1}.

Neutral-minus-Cation FTIR Difference Spectra. In contrast to anion formation of [M]-BChla and [M]-OH-BChla, cation formation results in an upshift of the FTIR absorption and difference bands for the carbonyl group frequencies. Parts c and d of Figure 3 show the representative absorption and neutral-minus-cation difference spectra before and after oxidation to the cation of [Cu]-BChla. The peak positions of the main difference bands of all derivatives are listed in Table 2.

In the cation absorption spectrum of [Cu]-BChla, the ester band is shifted to higher frequencies. This results in a difference band at 1750(+)/1736(−) cm^{-1}. The 13^1-keto band is upshifted from 1690 cm^{-1} in the neutral species to 1720 cm^{-1} in the cation of [Cu]-BChla. The corresponding difference spectrum shows a difference band at 1718(+)/1690(−) cm^{-1}. The 3-acetyl band

Table 2. Frequencies of the FTIR Neutral minus Cation Difference Spectra of [M]-BChla and [M]-OH-BChla[a]

compound	13^2-ester	13^1-keto	3^1-acetyl	skeletal modes				C−H and C−N modes		
BChla[b]	1750(+)/1732(−)	1716(+)/1684(−)	1664(−)	1575(−)	1544(+)	1524(+)	1419(−)		1377(−)	1339(−)
[Mn]-OH-BChla	1752(+)/1738(−)	1706(+)/1680(−)	1652(−)	1578(−)	1552(+)	1512(−)	1414(−)	1390(+)	1364(−)	1330(−)
[Mn]-BChla	1748(+)/1724(−)	1702(+)/1678(−)	1648(−)	1574(−)	1548(+)	1510(−)	1414(−)	1390(+)	1364(−)	1328(−)
[Zn]-OH-BChla	1754(+)/1740(−)	1720(+)/1690(−)	1656(−)	1588(−)	1550(+)	1506(−)	1418(−)		1378(−)	1338(−)
[Zn]-BChla	1748(+)/1732(−)	1714(+)/1684(−)	1658(−)	1590(−)	1550(+)	1520(−)	1430(−)		1376(−)	1336(−)
[Cd]-OH-BChla	1754(+)/1740(−)	1716(+)/1686(−)	1654(−)		1566(+)	1520(+)	1414(−)	1392(+)	1372(−)	1336(−)
[Cd]-BChla	1748(+)/1734(−)	1712(+)/1684(−)	1658(−)		1564(+)	1520(+)	1418(−)	1394(+)	1372(−)	1338(−)
[Ni]-OH-BChla	1764(+),1754(+)/1744(−)[c]	1718(+)/1696(−)	1656(−)	1582(+)	1542(+)		1440(−)		1388(−)	1336(−)
[Ni]-BChla	1768(+),1750(+)/1728(−)[c]	1712(+)/1694(−)	1654(−)	1582(+)	1540(+)		1440(−)		1388(−)	1334(−)
[Co]-OH-BChla	1754(+)/1740(−)	1716(+)/1688(−)	1650(−)	1576(+)	1538(−)		1434(−)		1382(−)	1338(−)
[Co]-BChla	1748(+)/1734(−)	1714(+)/1684(−)	1646(−)	1576(+)	1544(−)		1438(−)		1386(−)	1338(−)
[Cu]-OH-BChla	1762(+)/1744(−)	1722(+)/1692(−)	1658(−)	1568(+)	1536(−)		1428(−)		1378(−)	1338(−)
[Cu]-BChla	1750(+)/1736(−)	1718(+)/1690(−)	1658(−)	1570(+)	1538(−)		1428(−)		1376(−)	1338(−)
[Pd]-OH-BChla	1754(+)/1742(−)	1712(+)/1696(−)	1656(−)	1578(+)	1536(−)		1434(−)		1388(−)	1340(−)
[Pd]-BChla	1756(+)/1742(−)	1722(+)/1696(−)	1658(−)	1586(+)	1534(−)		1434(−)		1388(−)	1342(−)

[a] All band positions are in inverse centimeters. [b] Data taken from ref 13e. [c] Superposition of two difference bands.

is decreased in intensity and shifted toward higher frequencies too. Since this upshift is superimposed by other absorption bands, only a negative difference band at 1658 cm^{-1} is observed in the difference spectrum. A notable feature in the frequency region between 1600 and 1400 cm^{-1} is a strong band at 1554 cm^{-1} and the decrease of the band in the cation absorption spectrum at 1538 cm^{-1} of the neutral species. The difference spectrum shows two positive bands at 1570 and 1554 cm^{-1} and a negative band at 1538 cm^{-1}. Below 1400 cm^{-1}, the three main absorption bands of the neutral species are also present in the cation spectrum with shifted band positions and altered intensities. The difference spectrum shows two negative bands at 1376 and 1338 cm^{-1} and a positive band at 1324 cm^{-1}.

The neutral-minus-cation difference spectra of all other examined derivatives, with the exception of the Ni, Co, and Mn derivatives, follow the described [Cu]-BChla difference spectrum. The 13^2-ester band and the 13^1-keto band are upshifted in the [M]-OH-BChla compared to those in [M]-BChla, but the spectra are otherwise similar.

In the difference spectrum of [Ni]-OH-BChla, the 13^2-ester band at 1764 cm^{-1} develops a shoulder at 1754 cm^{-1} (Figure 4b). In [Ni]-BChla, the main positive difference band is positioned at 1750 cm^{-1} with a shoulder at 1768 cm^{-1}. In the frequency region between 1600 and 1400 cm^{-1}, a strong positive difference band at 1542 cm^{-1} ([Ni]-OH-BChla) and 1540 cm^{-1} ([Ni]-BChla) is observed. The other frequency bands follow again the band pattern described above.

In the frequency region between 1600 and 1400 cm^{-1}, the Co derivatives show a strong, broad, unsplit band at 1576 cm^{-1}. The other bands follow the representative band pattern of [Cu]-BChla described above.

The Mn derivatives are oxidized at the central metal instead of at the ring system.[12] This results in altered skeletal difference bands (Figure 5b). A difference band at 1578(+)/1552(−) cm^{-1} is followed by a strong negative band at 1512 cm^{-1}. The residual bands bear a high similarity to the ones described for [Cu]-BChla.

Discussion

Three major effects are responsible for the generation of a difference band upon reduction or oxidation of [M]-BChla and [M]-OH-BChla. First, the bond strength in the conjugated system can be changed as a reaction of the charge redistribution occurring after reduction or oxidation. Second, the positive or negative charge can influence the bond order of bonds not involved in the conjugated system by the inductive effect. Finally, H bridges between the pigments and exogeneous ligands can be changed. Since we have chosen the aprotic solvent THF, we can exclude changes in H bridges upon the redox reactions, which otherwise can influence the band structure.

Neutral-minus-Anion FTIR Difference Spectra. The observed downshift of all carbonyl frequencies in the neutral-minus-anion difference spectra can be explained by a weakening of the double bond character of the carbonyl bonds. The redistribution of the electron charge density in the macrocycle upon reduction results in an increase in conjugation for the carbonyl groups, lowering the IR frequencies of these bands. Ballschmitter and Katz[17] showed that the 13^1-keto group is involved in conjugation; thus, a weakening of the double bond character seems possible for this carbonyl group. For the ester groups, one might not expect such an effect, since they are not involved directly in conjugation with the bacteriochlorin system. However, the ester difference band, which corresponds to a downshift by 14−26 cm^{-1}, indicates that either inductive Coulombic interaction or a direct coupling exerts considerable influence on one or both of the ester groups. The closer proximity of the 13^2-ester group to the conjugated ring system suggests that this ester group is at least partially involved in conjugation. This is confirmed by comparison of the FTIR neutral-minus-cation difference spectra of Chla[21] and BChla[22] with the difference spectra of the pyro compounds which lack the 13^2-ester group. The pyro compounds did not show a difference band around 1750(+)/1737(−) cm^{-1}. Consequently, this difference band must arise from the 13^2-ester group in the native pigments. The 17^2-ester group is essentially unperturbed by oxidation.

In general, the band frequencies of the 13^2-ester group and the 13^1-keto group are shifted toward higher frequencies for [M]-OH-BChla relative to the unsubstituted [M]-BChla. The same effect is also observed in RR studies for the 13^1-keto group of Chla and 13^2-hydroxy-Chla by Cotton and Heald.[23] An explanation for the upshifted carbonyl bands is disconnection of the possible keto−enol tautomerism through the 13^2-hydroxy group. This should lead to stronger carbonyl bonds, causing an upshift in the 13^2-ester and 13^1-keto band.

A striking feature of the absorption spectra of the neutral species of the Ni derivatives is a split or broadened ester band. Furthermore, the neutral-minus-anion difference spectra show an upshift ([Ni]-OH-BChla) or the superposition of two difference bands ([Ni]-BChla) for the 13^2-ester difference band. This

(21) Nabedryk, E.; Leonhard, M.; Mäntele, W.; Breton, J. *Biochemistry* **1990**, *29*, 3242.

(22) Leonhard, M.; Wollenweber, A.; Berger, A.; Kléo, J.; Nabedryk, E.; Breton, J.; Mäntele, W. In *Techniques and New Development in Photosynthesis Research*; Barber, J., Ed.; NATO ASI Series; Plenum: New York; 1989; Vol. 168, p 115.

(23) Cotton, T. M.; Heald, R. L. *J. Phys. Chem.* **1990**, *94*, 3968.

can be related to the coexistence of different states of [Ni]-OH-BChla in THF solution as will be explained below in more detail. It is known from X-ray structure analysis that porphyrin systems like [Ni]-OEP (OEP = 2,3,7,8,12,13,17,18-octaethyl-21*H*,23*H*-porphyrin dianion) have deformed macrocycles instead of planar ones. [Ni]-OEP forms either orthorhombic[24] or triclinic crystals.[25] This difference in crystal structure leads to different RR spectra in the solid state.[26] In contrast to this, their RR spectra in solution are similar, leading to the conclusion that they have an identical structure. More recently, Anderson and co-workers[27] observed large line widths in the RR spectra of [Ni]-OEP in solution and attributed them to a coexistence of planar and nonplanar conformers in solution. Evidently, there exists a close balance between the loss of conjugation by deformation of the macrocycle and the gain in the metal–nitrogen bond strength in the distorted structure. Distorted structures are observed in complexes with metal–nitrogen bonds shorter than 2.01 Å, a value estimated by Hoard[28] for an unconstrained planar porphyrin. Furthermore, raising the temperature favors a structure that is distorted slightly toward the nonplanar form.[29] The value of the Ni–N distance for [Ni]-OH-BChla, determined by an extended X-ray absorption fine structure (EXAFS) study, is 1.95 ± 0.02 Å.[30] Unfortunately, up to now there were no X-ray structures of BChla. The only reported structures are those of methylbacteriopheophorbide *a*,[31] BChl *d*,[32] [Ni]-hydroporphyrins,[33] and substituted [Ni]-Por.[34] Nevertheless, all these X-ray structures point out a remarkable flexibility of the macrocycle, indicating that the isocyclic ring V, the central metal, or the reduced double bonds in hydroporphyrins contributed to the observed flexibility. This is also pointed out in a RR study of [Ni]-methylpyropheophorbide *a*.[35]

The flexibility of the macrocycle also seems to exist in the case of [Ni]-OH-BChla if judged from the visible absorption spectra. Hartwich et al.[11] observed unusually strong circular dichroism (CD) of the [Ni]-OH-BChla in diethyl ether, dioxane, or acetonitrile, where the Q_x maximum is located at ~530 nm. This is assigned to a tetracoordinated Ni central metal with substantial distortion of the macrocycle. Solvent change to pyridine shifts the Q_x absorption to ~600 nm and simultaneously decreases the CD intensity to the "normal magnitude" of other [M]-BChla derivatives, indicative of an almost planar macrocycle. Comparison with the data for the Q_x shifts of other [M]-BChla upon the same solvent change together with ^{1}H NMR data in these solvents leads to the conclusion that [Ni]-OH-BChla is hexacoordinated in pyridine.

It was concluded that the energy of the Q_x band of [M]-BChla can be used as an indicator of the coordination number of the central metal with the rough estimate that a change of the coordination number by +1 is accompanied by the decrease of the Q_x transition energy of ~1000 cm^{-1}. This would mean that pentacoordinated [Ni]-OH-BChla in solution should have a Q_x absorption around 560 nm. Although we were not able to find a suitable solvent in which [Ni]-OH-BChla shows the expected absorption behavior for penta-coordination, there is EXAFS evidence for its existence when the pigment is incorporated into the binding sites for B_A and B_B of bacterial reaction centers. Here, pentacoordinated [Ni]-OH-BChla shows a Q_x absorption at ~585 cm^{-1}.[30]

It is also known that the reaction center protein environment produces a red shift for the pigment Q_x absorptions of ~700 cm^{-1} as compared to identically coordinated pigments in solution,[9c] yielding the expected 565 nm Q_x absorption in solution. The CD spectra for [Ni]-OH-BChla in the reaction center protein matrix give no hint of a substantial distortion of the macrocycle with pentacoordinated Ni.

On the basis of this argument, we attribute the main Q_x absorption band of [Ni]-OH-BChla in THF (~530 nm) to a tetracoordinated Ni complex, and the shoulder at ~565 nm to a more planar pentacoordinated species coexisting in solution.

A deformation of the ring system should result in a further decreased conjugation of the 13^2-ester group and the 13^1-keto group with the ring system. This results is an upshift of these bands in the IR absorption and difference spectra. The split 13^2-ester absorption band of [Ni]-OH-BChla can thus be attributed to a coexistence of a distorted, tetracoordinated (band at 1746 cm^{-1}) and a planar, pentacoordinated (band at 1732 cm^{-1}) species in solution. This explanation also holds for [Ni]-BChla, although only a broadened 13^2-ester absorption band is observed, thus indicating that the 13^2-hydroxy group shifts the equilibrium in solution toward the nonplanar species.

In the frequency region between 1400 and 1600 cm^{-1}, the IR difference bands are less intense. Anion formation results in substantial shifts since the redistribution of the π-electrons influences most of the skeletal vibrations. An analysis of these shifts for the monoanions of [M]-OEiBC (OEiBC = 2,3,7,8,-12,13,17,18-octaethyl-21*H*,23*H*-isobacteriochlorin dianion) showed that these bands shift up or down depending on the electronic properties of the macrocycle.[36]

In the frequency region below 1400 cm^{-1}, all difference spectra obtained bear a close resemblance. We observed three positive bands between 1300 and 1400 cm^{-1} in the difference spectra of all derivatives, indicating a change in bond order for the C–N and C–H vibrations. These difference bands are also reported for BChla at approximately the same positions. This suggests that these difference bands are unaffected by transmetalation and thus are due to either a C–N or a C–H vibration without contributions from C_α–C_m stretching modes. The C_α–C_m stretching modes should be sensitive to transmetalation like the other skeletal vibrations. This view is supported by the band assignments of Lutz for BChla.[37]

Neutral-minus-Cation Difference Spectra. All difference spectra of the cation species of [M]-BChla and [M]-OH-BChla show an upshift of the bands in the carbonyl frequency region between 1600 and 1770 cm^{-1}. The large perturbation observed for the carbonyl frequencies appearing in this region upon oxidation can be related to a lowered charge density in the

(24) Mayer, E. F., Jr. *Acta Crystallogr., Sect. B* **1972**, *28*, 2162.
(25) Cullen, D. L.; Mayer, E. F., Jr. *J. Am. Chem. Soc.* **1974**, *96*, 2095.
(26) Spaulding, L. D.; Chang, C. C.; Yu, N.-T.; Felton, R. H. *J. Am. Chem. Soc.* **1975**, *95*, 2517.
(27) Anderson, K. K.; Hobbs, J. D.; Luo, L.; Stanley, K. D.; Martin, J.; Quirker, E.; Shelnutt, J. A. *J. Am. Chem. Soc.* **1993**, *115*, 12346.
(28) Hoard, J. L. In *Porphyrins and Metalloporphyrins*; Smith, K. M., Ed.; American Elsevier: New York, 1975; p 317.
(29) Kim, D.; Miller, L. A.; Rakhit, G.; Spiro, T. G. *J. Phys. Chem.* **1986**, *90*, 3320.
(30) Chen, L. X.; Wang, Z.; Hartwich, G.; Katheder, I.; Scheer, H.; Tiede, D. M.; Scherz, A.; Montano, P. A.; Norris, J. R. *Chem. Phys. Lett.* **1995**, *234*, 437.
(31) (a) Barkigia, K. M.; Fajer, J.; Smith, K. M.; Williams, G. J. B. *J. Am. Chem. Soc.* **1981**, *103*, 5890. (b) Barkigia, K. M.; Gottfried, D. S.; Boxer, S. G.; Fajer, J. *J. Am. Chem. Soc.* **1989**, *111*, 6444.
(32) Smith, K. M.; Goff, D. A.; Fajer, J.; Barkigia, K. M. *J. Am. Chem. Soc.* **1982**, *104*, 3747.
(33) (a) Kratky, C.; Waditschatka, R.; Angst, C.; Johansen, J. E.; Plaquevent, J. C.; Schreiber, J.; Eschenmoser, A *Helv. Chim. Acta* **1985**, *68*, 1312. (b) Smith, K. M.; Goff, D. A. *J. Am. Chem. Soc.* **1985**, *107*, 4954. (c) Barkigia, K. M.; Tompson, M. A.; Fajer, J.; Pandey, R. K.; Smith, K. M. Vicente, M. G. H. *New J. Chem.* **1992**, *16*, 599. (d) Barkigia, K. M.; Fajer, J. In *The Photosynthetic Reaction Center*; Norris, J. R., Ed.; Academic Press: San Diego, 1993; Vol. 2, p 513. (e) Renner, M. W.; Furenlid, L. R.; Barkigia, K. M.; Forman, A.; Shim, H.-K.; Simpson, D. J.; Smith, K. M.; Fajer, J. *J. Am. Chem. Soc.* **1991**, *113*, 6891.
(34) Barkigia, K. M.; Renner, M. W.; Furenlid, L. R.; Medforth, C. J.; Smith, K. M.; Fajer, J. *J. Am. Chem. Soc.* **1993**, *115*, 3627.
(35) Senge, M. O.; Smith, K. M. Photochem. Photobiol. **1991**, *54*, 841.
(36) Procyk, A. D.; Stolzenberg, A. M.; Bocian, D. F. *Inorg. Chem.* **1993**, *32*, 627.
(37) Lutz, M. In *Advances in Infrared and Raman spectroscopy*; Clark, R. H. J., Hester, R. E., Eds.; Wiley: Heyden, 1984; Vol. 11, p 211.

macrocycle. This loss in charge density decreases the conjugation of the carbonyl bonds and thus increases the band frequencies. This holds for both the 13^2-ester group only partially conjugated to the bacteriochlorin system as well as the directly conjugated 3-acetyl and 13^1-keto groups. The observed upshifts are in general agreement with the difference spectra reported for BChla[13e] and Chla.[13b]

The 13^2-hydroxy group has the same influence on the neutral-minus-cation difference spectra as on the neutral-minus-anion difference spectra. The upshift for the 13^2-ester difference band is in the same range (about 4−8 cm^{-1}) in both the neutral-minus-anion and neutral-minus-cation difference spectra. This indicates that this shift is not due to a perturbed charge density in the anion or cation species of the [M]-OH-BChla relative to the [M]-BChla. It can be rationalized as the inhibition of the possible keto−enol tautomerism (see above).

The positive part of the 13^2-ester difference band in the Ni derivatives is composed of two superimposed bands. As discussed above, we presume that this is due to the coexistence of a nonplanar, tetracoordinated and a planar, pentacoordinated species in solution.

The difference bands between 1600 and 1400 cm^{-1} are composed of the coupled stretching modes of the bacterioclorin macrocycle. As mentioned in the preceding section, upshifts and downshifts of the absorption bands upon π-radical formation are observed in this frequency region. The Ni and, to a minor extent, the Co derivatives did not follow the general band pattern, which can again be attributed to a deformation of the macrocycle, either in the neutral species or upon cation formation. The skeletal modes should be most strongly influenced by such a deformation. This is in agreement with the electrochemical data.[12] The redox potentials for the first oxidation step are lowered for the Ni and Co derivatives in contrast to the other species. This can be explained by a distortion of the ring system. This should influence the molecular orbitals involved in oxidation, thus leading to a lowering of their energy.

Below 1400 cm^{-1}, all neutral-minus-cation spectra exhibit the same band pattern with only small wavelength variations among the different pigments. This is an indication that the modes in this frequency region are unaffected by transmetalation. Thus, they must be composed primarily of C−H and C−N vibration modes, as observed with the anion-minus-neutral difference spectra.

FTIR Difference Spectra with [M]-BChla Undergoing Metal-Centered Redox Processes. In our electrochemical paper,[12] it was shown that reduction occurs at the central metal rather than at the macrocycle π-system of the Co derivatives. The same holds for the oxidation of the Mn derivatives. It is remarkable that the Co and Mn derivatives exhibit, in general, the same down- (Co) or upshifts (Mn) in the difference spectra for the carbonyl frequencies and below 1400 cm^{-1} as do the other [M]-BChla and [M]-OH-BChla. In contrast to this, the skeletal modes are different compared to the other derivatives. This must be due to an altered charge redistribution in the conjugated ring system upon oxidation or reduction of the central metal.

We also obtained the difference spectrum of the dication [Mn(III)]-OH-BChla$^{\bullet+}$, where Mn(II) is first oxidized to Mn(III) and the bacteriochlorin ring subsequently to the π-cation radical. The FTIR difference spectra show for the second step a further upshift of the carbonyl bands due to an even more decreased conjugation of these groups with the macrocycle. The band pattern corresponds to that of the other cation species. The influence of the second oxidation step on the bands in the region below 1400 cm^{-1} is only minor as is the influence of the π-cation radical formation in all other pigments (see above). This further supports our presumption that the metal sensitive $C_\alpha-C_m$ stretch does not contribute to the C−N and C−H modes in this region.

Conclusions

Three classes of FTIR difference spectra are observed. [M]-BChla (M = Zn, Cd, Cu, Pd, Mn(II)) show normal difference spectra with a band pattern close to that of the parent compound BChla. Difference spectra with [M]-BChla undergoing metal-centered processes (M = Co, Mn) show strong deviations from the normal spectra in the frequency region between 1600 and 1400 cm^{-1}. The third class of difference spectra resemble the normal spectra, but the skeletal modes are strongly different from the normal behavior (M = Co(II), Ni) in the π-cation difference spectra. This can be attributed to a deformation of the macrocycle.

Generally, reduction leads to a downshift in the carbonyl frequencies, whereas oxidation leads to an upshift. This can be explained in terms of the effect of a redistribution of the π-charge density in the macrocycle on the carbonyl bond order: it is decreased by an increased electron density, and vice versa.

Substitution of the 13^2-hydrogen for the hydroxy group results in an upshift of the 13^2-ester difference band in both the neutral-minus-anion and neutral-minus-cation difference spectra. This is most likely due to the inhibition of the possible keto−enol tautomerism, including a partial enolization of the β-ketoester system in [M]-BChla.

This upshift of the 13^2-ester difference band is increased for the Ni derivatives in the difference spectra. If we combine the electrochemical and spectroelectrochemical measurements,[12] the CD and UV/vis measurements,[11] and the EXAFS study[30] of the Ni species, this band upshift can be attributed to a distortion of the macrocycle from planarity. This deformation is already present in the neutral species, as indicated by the split or broadened ester absorption bands. Thus, in solution there is a coexistence of a distorted, tetracoordinated and a planar, pentacoordinated species.

The deviation of the bands in the neutral-minus-cation difference spectra in the skeletal frequency region for the Ni and Co derivatives compared to the other species can also be attributed to a deformation of the macrocycle. The 13^2-ester absorption and difference bands therefore appear to be a structural marker for out-of-plane distortions of the macrocycle in [M]-BChla systems.

In the Co and Mn derivatives, redox processes occur at the central metal. Only the skeletal modes show different responses; they can therefore be used as marker bands to distinguish the site of the redox reaction. The metal-centered redox processes have the same effect on the carbonyl group frequencies as the ring-centered redox processes.

Acknowledgment. This work was supported by the Deutsche Forschungsgemeinschaft (DFG) "Graduiertenkolleg für ungepaarte Elektronen in Chemie, Physik und Biologie" to C.G., J.H., and W.M. and "Sonderforschungsbereich 143, TPA 9" to G.H. and H.S. W.M. was funded by DFG through several grants and by a Heisenberg fellowship. G.H. acknowledges a graduate fellowship from the "Freistaat Bayern". Financial support from the Fonds der Chemischen Industrie is gratefully acknowledged. We thank S. Grzybek for help with the computer program for potentiostat and spectrophotometer control.

JA944183Z